

EXPERIMENTAL STUDIES OF HIGH VISCOSITY OIL-WATER (WATER-ASSIST) FLOW BEHAVIOR IN HORIZONTAL PIPE

Solomon O. Alagbe

Department of Chemical Engineering, Faculty of Engineering and Technology,
Ladoke Akintola University of Technology, P.M.B.4000, Ogbomoso –Nigeria

Email: alagbeuk@yahoo.co.uk; soalagbe@lautech.edu.ng

ABSTRACT

The challenges of low oil production due to the flow assurance problems associated with transportation of high viscosity oil in pipes has attracted attentions for more than two decades. Laboratory scale studies were conducted on co-current flow of high viscosity oil and water in a horizontal perspex pipe 1-in ID 5m long. Two oil brand, CYL680 and CYL1000, 917 and 916.2kg/m³ densities and viscosities 1.830 and 3.149Pa.s at 25°C respectively were used. The interfacial tension of high viscosity oil/water is 0.026N/m at 19°C. The results show the reduction pressure gradient by one order of magnitude. The flow patterns identified from the trend plot of the downstream pressure signals, its probability density function (PDF) and statistical moments as well as visualisation of the flow are Water Assist- Annular (WA-ANN), Dispersed Oil in Water (DOW/OF), Oil Plug in Water (OPW/OF) with oil film on the wall and Water Plug in Oil (WPO). Thin layer of wavy oil film was on the pipe wall forming an envelope for water in all the flow patterns where water was the continuous phase.

Keywords: Core annular flow, co-current flow, probability density function (PDF), Water-Assisted (WA) flow

Introduction

In the petroleum industry, mixtures of oil and water are transported in pipes over a long distance and accurate prediction of such multiphase flow characteristics, such as the desired flow pattern, water holdup, pressure gradient and flow stability are important in many engineering applications. In spite of their importance, these characteristics have not been thoroughly explored to the same extent on heavy oil related flows as they have been explored in light-oil related flows. Low production of heavy oils is known to be bedeviled by high viscosities (Dusseault, 1993, 1995). Beson (2005) and Owen et al. (2010) amongst many researchers reported that transportation of heavy oil (high viscosity oil) is energy intensive, hence different methods are being proposed to alleviate this problem. Cold Heavy Oil Production (CHOP) is among low energy consuming methods proposed but its application requires a proper understanding of the phenomenon.

Despite the fact that a good number of work has been done on the characterisation of oil flows in pipes, attention has been on conventional oil which covers low and medium viscosity oils (<1000cP) (Barnea et al. (1980), Martinez et al. (1988), Brauner et al. (1992), Trallero et al. (1997), and Angeli and Hewitt (2000) while a paucity of information exist on unconventional oil i.e. the high viscosity oils. The outcomes of the difference

in the fluid properties, (most especially, the viscosity) has thrown a caution on the reliance and application of the existing knowledge. Several researchers have attempted the classification of the two-phase gas-liquid flow patterns by using the sensor response because it is objective. The fluctuations of local absolute and differential pressures were found to be regime-dependent and the statistical characteristics (power spectral density, probability density function, and auto and cross-correlation functions) are useful for the flow pattern classification Santoso et al. (2012). This is expected to be cost effective for oil and gas industries because the required online pressure data are already being used. However, this method is yet to be established for oil-water flow in horizontal pipes.

In theory, core annular flow (CAF) pattern was proposed for transporting high viscosity oils in order to overcome the flow assurance problem observed by the earlier researchers, prescribing that CAF must have water wetting the wall and the pressure gradient shall be that of the fluid wetting the pipe wall. Joseph et al. (1997) reported an increased in pressure gradient due to fouling caused by the presence of wax when CAF approach was applied in the field. Hence, research foci of subsequent researches were fouling prevention (Arney et al. (1996), Angeli and Hewitt (1999)). The possibility of water retention on pipe wall however has not been achieved. Therefore this

paper presents a recent investigation on flow behaviours of oil-water over a range of high viscosities by examining the effects of water flow on pressure gradient and also the outcome flow patterns by comparing visualisation and pdf approaches.

Experimental setup

The test section was made up of 1-in ID of a 5.5m long transparent acrylic horizontal pipe. The pressure taps were positioned at 2.93m and 5.10m, while differential pressure taps were placed at 2.92m and 5m. Temperature transducers were also at 0.7m, 1.87m and on the test section. The schematic diagram of the rig is as shown in Figure 1.

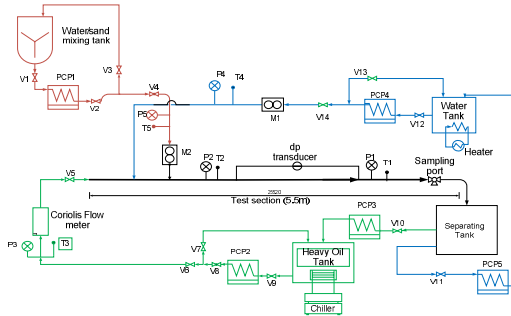


Figure 2: Schematic of 1-inch four phase transport facility at Cranfield University PASE laboratory

Labview software of National Instruments was used to record voltages through a computer which were converted by calibration to the desired parameters. An application was created and data were taken every 0.004 seconds over 30 seconds for each run. The pressure drop was measured between a pair of taps 2.17 m apart where the first tap was at a distance of 2.155 m from the inlet. A differential pressure transmitter (Honeywell STD120) was used for this purpose. The transducer has a least count of 1.0×10^{-2} Pa and an accuracy of $\pm 0.05\%$ under the experimental conditions. The static water head has been used along with differential pressure drop $(dp)_{diff}$ as obtained from the transmitter to extract the total pressure drop. The tubing system of the differential pressure transducer was always purged after each experimental run. A (DSCH9, SONY) video recorder is used for clip recording of the flow phenomena at different superficial velocities of both the phases at a distance 3.0 m away from the inlet. The relevant properties of the two fluids (oil

and water) used in the simulation are as given in Table 1.

Table 3: Fluid properties used for the Experimentation

Fluid	Density @25°C (kg/m ³)	Viscosity @25°C (Pa.s)	Surface Tension @19°C (N/m)
Water	998.2	0.001003	0.026
Oil	916.2	3.149	

Results and Discussion

Pressure gradient

The pressure gradient profile against water cut and superficial velocities of water (V_{sw}) for different oil viscosities are as presented in Figure 3 to Error! Reference source not found.5. Generally, it could be observed that the pressure gradient values are directly proportional to the oil flow rate (i.e. high oil flow rate has a relatively high pressure gradient). Considering each trend in Figure 3 and Error! Reference source not found.3, the pressure gradients were first observed to decrease from the high value corresponding to single phase oil gradients (i.e. at zero water cut where the flow was reduced to single phase oil) to the lowest pressure gradient attainable in each oil flow rate considered in the experiments. After reaching the lowest point, the pressure gradient starts to climb. For example, the lowest pressure gradients attained for 3300cP are 1.54, 1.23 and 2.95 kPa/m when the V_{so} were 0.06, 0.2 and 0.55m/s respectively. The increase observed in pressure gradients were also observed to be a function of the increase in the water cut in each of the three scenarios. In summary, the pressure gradient first fell until a minimum was reached and then rose with increase in water cut. It was equally observed that the lowest gradients being discussed here occurred mostly at low water cuts which suggests that the low water cuts are needed to lower the oil-wall friction, while high water cut (after the friction has been reduced to minimum) aids the dispersion of oil and then its transfer back to the pipe wall, which perhaps lead to increase in the wall shear stress. It could also be seen from these figures that the pressure drop reduction of heavy oil is not dependent of viscosity because all the gradients are reduced by at least an order of magnitude.

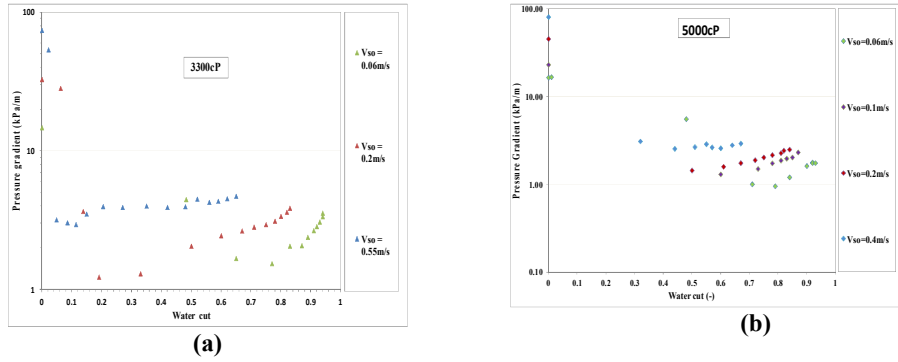


Figure 3: Comparison of pressure gradient of oil-water flow for Various nominal oil viscosity at different oil superficial velocities and water cut

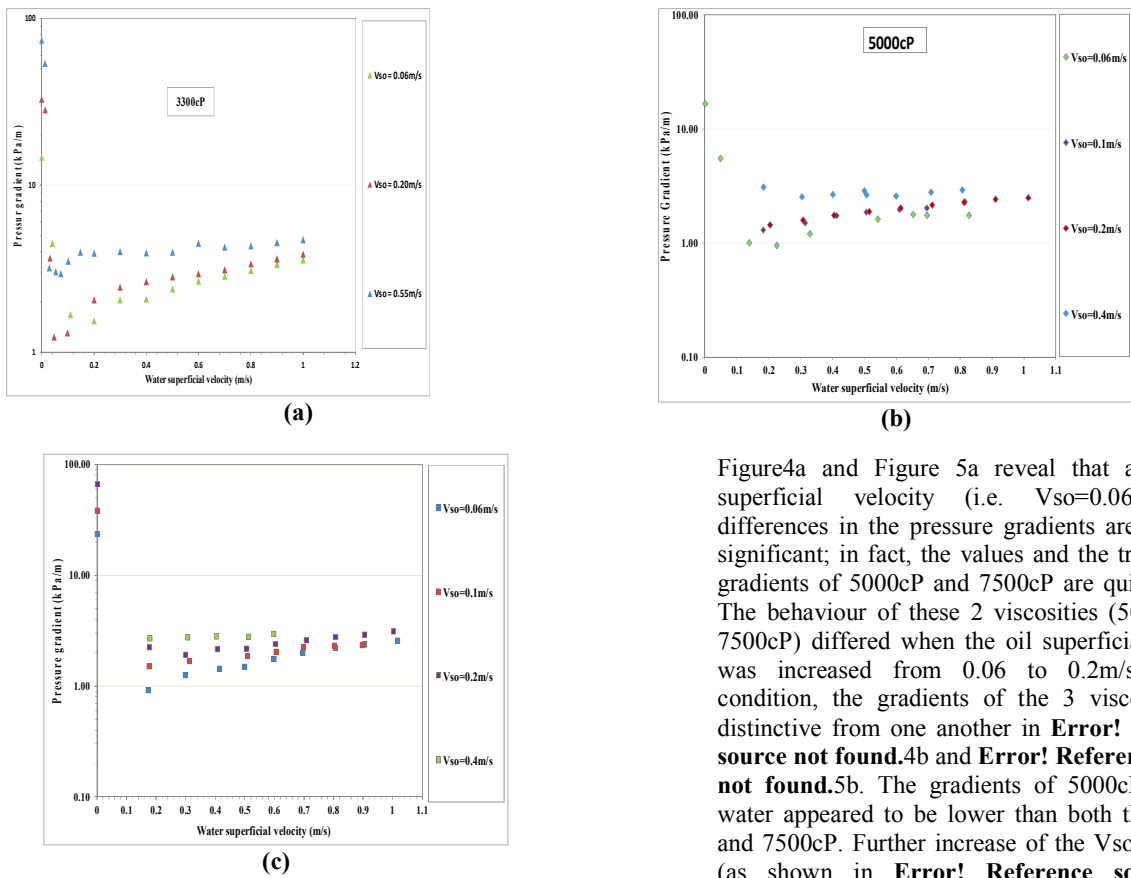


Figure 4: Comparison of pressure gradient of oil-water flow for Various nominal oil viscosity at different oil and and water superficial velocities

The comparison of the pressure gradients of different oil viscosities to expose the specific behaviour of the oil viscosities considered in this research are as presented in Figure 4. Generally, the gradients of 3300cP oil with water appeared higher than both 5000 and 7500cP. In this research,

Figure 4a and Figure 5a reveal that at low oil superficial velocity (i.e. $V_{so}=0.06\text{m/s}$) the differences in the pressure gradients are not quite significant; in fact, the values and the trend of the gradients of 5000cP and 7500cP are quite similar. The behaviour of these 2 viscosities (5000cP and 7500cP) differed when the oil superficial velocity was increased from 0.06 to 0.2m/s; at this condition, the gradients of the 3 viscosities are distinctive from one another in **Error! Reference source not found.4b** and **Error! Reference source not found.5b**. The gradients of 5000cP oil with water appeared to be lower than both the 3300cP and 7500cP. Further increase of the V_{so} to 0.4m/s (as shown in **Error! Reference source not found.4c** and **Error! Reference source not found.5c**) show that 3300cP oil flow with water gives the lowest gradients compare to 5000cP and 7500cP oils. In addition, both the gradients of 5000cP and 7500cP are virtually the same on the high side of the water cut or V_{sw} . This behaviour is quite unique and has not been reported by any researcher. This behaviour is not understood at the moment; hence, more investigation is needed to verify this behaviour.

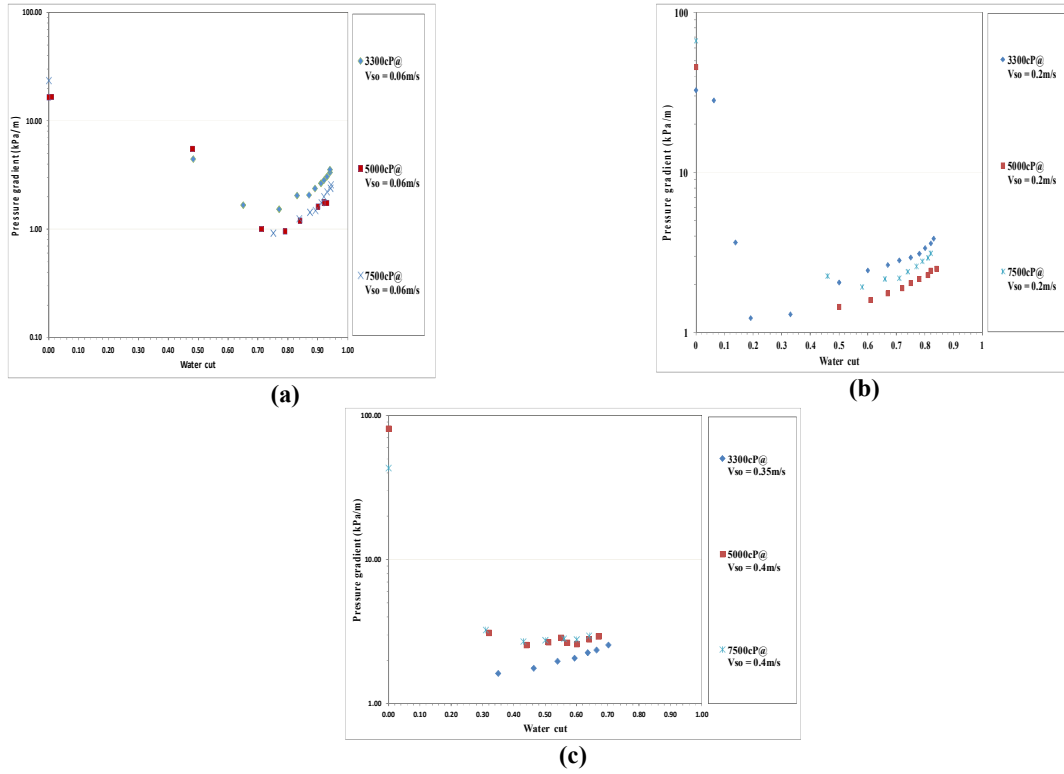


Figure 4: Effect of viscosity on pressure gradient various oil superficial velocities and different water cut

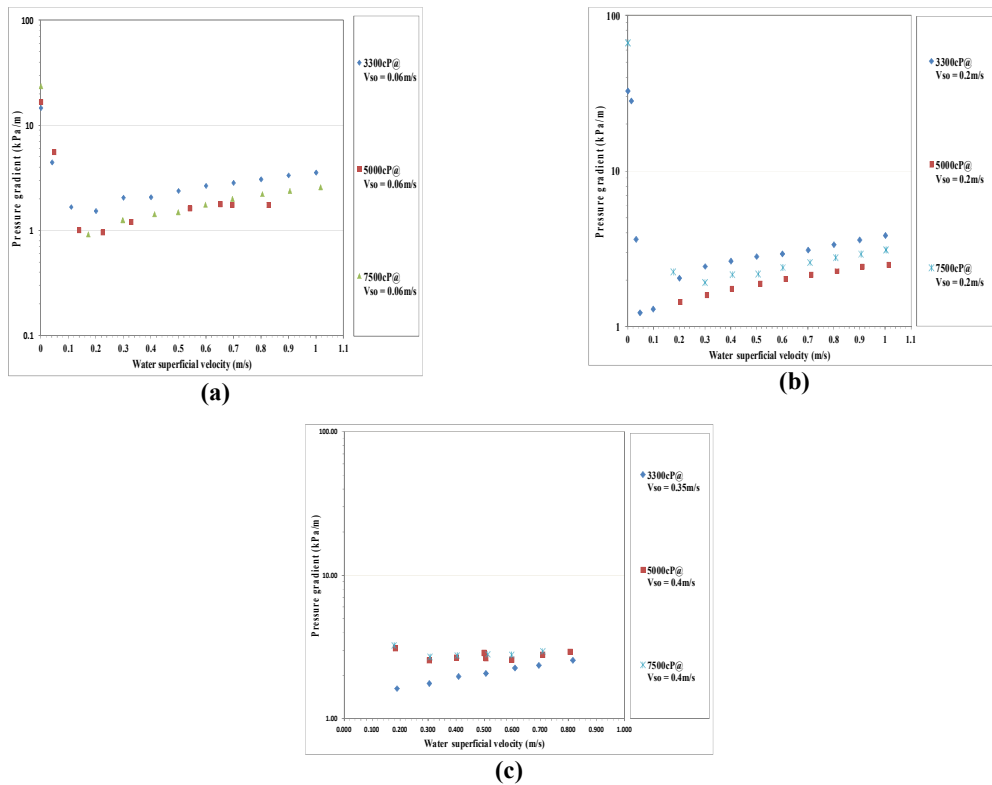


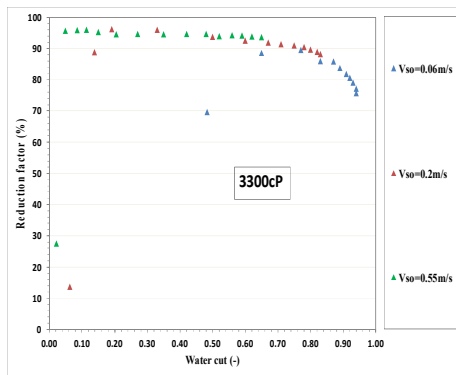
Figure 5: Effect of viscosity on pressure gradient at various oil superficial velocities and different water superficial velocity

Reduction factor

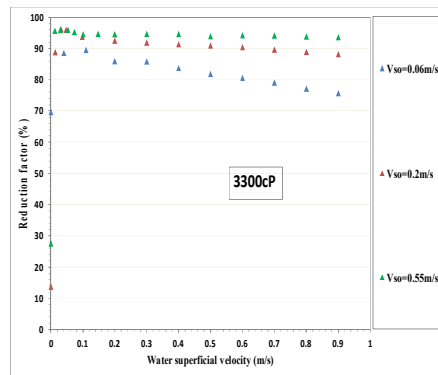
In order to quantify the effect of water assistance in the transport of heavy oil through a channel, the ratio of the frictional pressure gradient of single phase oil flow through a channel to the frictional pressure gradient of two-phase oil-water flow through the same channel, known as the reduction factor is employed. It was observed from the

Figure 65 and Error! Reference source not found.6b that the degree of the reduction of the pressure gradient, firstly increases and then decreases with the increase in water cut. In other words, when the water cut becomes too low, the effect of water on the reduction of the pressure

gradient is also low. For instance, when the oil superficial velocity was 0.2 and 0.55m/s with the water cut at 0.06 and 0.02 respectively, the reduction factor are about 13 and 27%. The highest pressure gradient reduction factors attained in the three scenario investigated occur at different point that could be referred to as optimum water cut for each respective oil flow rate considered in the test. It is also worthy to note that the reduction factors keep decreasing as water cut continues to increase. This was evident at low V_{so} , i.e. 0.06m/s. These data agree with the behaviour obtained by other researchers’ (Sotgia et al., (2008); Bensakhria et al., (2004); Strazza et al., (2011))



(a) water cut



(b) water superficial velocity

Figure 65: Pressure gradient reduction factor against water cut and water superficial velocity of oil-water flows at 3300cP oil viscosity (nominal)

Flow regime identification

The flow regime identification studies are presented in this section using visualisation (i.e. subjective) and pressure signal trend and PDF analysis (i.e. objective) approaches. Samples of the observed oil-water flow configurations are presented to illustrate the flow patterns obtained in the course of the experiments. The flow pattern images are captured from both side and bottom views of the pipe.

Flow regime identification by visualisation

The observed flow patterns are presented as a set of photographs in

Table 4,

Table 5 and

Table 6. Generally, an oil coated wall was observed in all the oil-water flow cases. These coatings appeared wavy on the wall; which suggests that the oil film thickness on the wall was not uniform. It was also observed that this oil coating was affected by the water cut, demonstrated by increased wall transparency as the water cut increased.

At a low oil superficial velocity (V_{so}) of 0.06m/s for 3300cP nominal oil viscosity, plug flow of the oil-phase in water with oil film (OPW/OF) coating the wall was observed when water superficial velocity (V_{sw}) was 0.2m/s. This plug flow continues until V_{sw} reached 0.4m/s. These oil plugs flew along the upper part of the pipe wall as a result of buoyancy/lift force acting on the oil. As the V_{sw} increased from 0.40m/s, this oil plug became streak-like and dispersed in water known as dispersed oil in water (DOW/OF). It was further observed that the higher the V_{sw} the more dispersed the oil in this case (where V_{so} equals 0.06m/s). However, the flow pattern observed when the V_{so} was increased to 0.20m/s and the V_{sw} was 0.20m/s is called water-assist annular (WA-ANN) flow which is a variant of the core annular flow. In this WA-ANN flow, the oil flows in a continuous manner in the core of the pipe being surrounded by water but with oil film on the pipe wall while CAF does not have oil film on the pipe wall. This WA-ANN flow appeared like

bamboo wave when the V_{sw} was 0.20m/s. The annular oil flow in the core began to break when the V_{sw} increased beyond 0.50m/s. In this case also, it was observed that the core thickness (diameter) was reducing as the water cut increased.

From this experiment it was found that CAF pattern is not feasible; this is because it has not been possible to prevent the pipe wall from being fouled by oil. However, the oil in the core of the pipe could still be continuous and increase in diameter with increase in oil flow rate. This is justified by

Table 6 where V_{so} is 0.55m/s. The WA-ANN continues to exist with increase in V_{sw} , although the core diameter was decreasing with respect to the increase in V_{sw} . From the foregoing, it could be inferred that the increase in V_{so} and/or decrease in V_{sw} (or water cut) promotes WA-ANN flow while the reverse promotes other intermittent flows i.e. OPW/OF and DOW/OF.

Additional flow behaviour observed in this study is the swirl type of oil and water flow as shown in Table 7; this behaviour is not continuous throughout the pipe and it is not local to a specific location in the pipe. This was observed to emerge between the oil continuous and water continuous flow. It is difficult to classify this as a stable flow pattern but a transition between oil and water continuous flow condition.

Table 4: Oil-water flow pattern at 0.06m/s oil superficial velocity

Flow conditions	Pictures	Flow regime
$V_{so}=0.06\text{m/s}$ $V_{sw}=0.2\text{m/s}$ $wc = 0.77$		OPW/OF
$V_{so}=0.06\text{m/s}$ $V_{sw}=0.3\text{m/s}$ $wc = 0.83$		OPW/OF
$V_{so}=0.06\text{m/s}$ $V_{sw}=0.4\text{m/s}$ $wc = 0.87$		OPW/OF
$V_{so}=0.06\text{m/s}$ $V_{sw}=0.5\text{m/s}$ $wc = 0.89$		DOW/OF
$V_{so}=0.06\text{m/s}$ $V_{sw}=0.6\text{m/s}$ $wc = 0.91$		DOW/OF

$V_{so}=0.06\text{m/s}$
 $V_{sw}=0.8\text{m/s}$
 $w_c = 0.93$



DOW/OF

$V_{so}=0.06\text{m/s}$
 $V_{sw}=1.0\text{m/s}$
 $w_c = 0.94$



DOW/OF

Table 5: Oil-water flow pattern at 0.2m/s oil superficial velocity

Flow conditions	Pictures	Flow regime
$V_{so}=0.2\text{m/s}$ $V_{sw}=0.2\text{m/s}$ $w_c = 0.50$		WA-ANN
$V_{so}=0.2\text{m/s}$ $V_{sw}=0.5\text{m/s}$ $w_c = 0.71$		WA-ANN
$V_{so}=0.2\text{m/s}$ $V_{sw}=0.8\text{m/s}$ $w_c = 0.80$		DOW/OF
$V_{so}=0.2\text{m/s}$ $V_{sw}=1.0\text{m/s}$ $w_c = 0.83$		DOW/OF

Table 6: Oil-water flow pattern at 0.55m/s oil superficial velocity

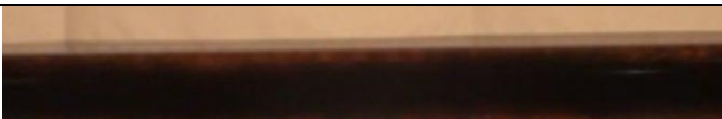
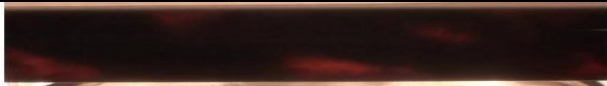
Flow conditions	Pictures	Flow regime
$V_{so}=0.55\text{m/s}$ $V_s=0.2\text{m/s}$ $w_c = 0.27$		WAVY WA-ANN
$V_{so}=0.55\text{m/s}$ $V_s=0.3\text{m/s}$ $w_c = 0.35$		WA-ANN
$V_{so}=0.55\text{m/s}$ $V_s=0.4\text{m/s}$ $w_c = 0.42$		WA-ANN
$V_{so}=0.55\text{m/s}$ $V_s=0.6\text{m/s}$ $w_c = 0.52$		WA-ANN
$V_{so}=0.55\text{m/s}$ $V_s=0.8\text{m/s}$ $w_c = 0.59$		WA-ANN
$V_{so}=0.55\text{m/s}$ $V_s=1.0\text{m/s}$ $w_c = 0.65$		WA-ANN

Table 7: Sample of additional oil-water flow pattern

Title	Flow description
SWO	

Flow regime identification by trend and PDF plot of pressure signals

The experiments carried out covered V_{so} ranging from 0.06 to 0.55m/s, and V_{sw} ranging from 0.01 to 1.0m/s. The V_{sw} was varied from a high to a low value, while keeping the V_{so} constant. Subsequently, the water velocity was reduced to the lowest value, and the experiments were repeated for other V_{so} . The pressure-time series were obtained from the pressure tap downstream of the test section for analysis of the flow pattern in the pipe. In order to compare and classify the PDF output of the pressure signals, and some video graphs were taken concurrently. The trend and PDF plots of oil-water flows for nominal oil viscosity 3300cP at V_{so} equals 0.06m/s is as presented on Table 8 using normalised pressure data. Trend plot and PDF are established methods for time series analysis of random signals. Table 8 together with

Table 4 were compared to draw inferences of the flow patterns, in addition to some established researches in the literatures.

The trend plots of the low water flow rates in Table 8 (where $V_{so}=0.06$ m/s, and $V_{sw} = 0.05, 0.10$ and 0.11 m/s) were obtained when the flows appeared to be dominated by oil phase and these justify and compared with McKibben's (2000) explanation as shown in

Figure 7. In their investigation of horizontal well heavy oil-water flows in 2-in ID, 12.7m long in which the oil viscosity employed ranged from 325 to 11200cP, similar observation to those in the flow conditions mentioned above were made. This same pattern was referred to as water slug in oil by McKibben et al. (2000); they proposed this flow pattern from their observation of the behaviour of the anemometer voltage readings during their investigation of similar condition; they explained that the upstream pressure of the probe fell linearly with time as the slug entered the test section and remained very low for about 2 to 3 seconds and then rose as the slug exited the section. The anemometer voltage reading fell as the slug passed, indicating that the oil velocity at this region has become very low, that is, the oil is nearly stationary at this position in the presence of the water slug. When V_{sw} was increased from 0.11 m/s up to 1.0m/s with V_{so} at 0.06m/s, the plots obtained are stable fluctuating signals. The trend plot for these high water flow rates region are similar in all the

cases considered. This also corroborated the fluctuating gradient plot from McKibben's research as shown in Figure 8 when the V_{sw} increases.

In this region, intermittent flows, that is, OPW/OF and DOW/OF were observed when V_{so} equals 0.06m/s, and WA-ANN when V_{so} equals 0.2m/s and 0.55m/s as shown on Table 7. Many researchers have adopted both trend and PDF technique to identify the flow patterns of gas-liquid flow (Matsui, 1984,1986) using pressure fluctuations, and liquid-liquid flow (Jana et al.,2006a) using normalised voltage signals of light attenuation of photodiode sensor under different flow conditions and very low oil viscosity (i.e. 1.37cP). The PDF curves are quantified by means of statistical analysis namely, skewness, standard deviation and kurtosis. The skewness characterises the degree of asymmetry of the distribution around its mean. A negative skew value implies that the left tail is longer; the mass of the distribution is concentrated on the right of the figure and it has relatively few low values while positive skew implies the opposite. The kurtosis is a measure of whether the data are peaked or flat relative to a normal distribution. In other words, data sets with high kurtosis tend to have a distinct peak near the mean, decline rather rapidly, and have heavy tails while data sets with low kurtosis tend to have a flat top near the mean rather than a sharp peak. At low oil and water superficial velocities (i.e. $V_{so}=0.06$ and $V_{sw}=0.05$ m/s), the PDF has a peak at a high value of normalised pressure and a positive skewness, and comparing with the observed image during experiment (which appeared like single phase oil because the presence of water could not be seen), it indicates the existence of oil as the continuous phase, and bubbles of water in it as described by McKibben et al. (2000) in a similar investigation. This could be described as water bubbly/plug flow in oil (WPO). An increase in V_{sw} from 0.05m/s to 0.11m/s at the same V_{so} led to a reduction in the standard deviation, a drift of the skewness towards zero and lower kurtosis were obtained as a result of this thin distribution. Similar distribution was reported in the literature by Jana et al. (2006b), as a condition where no information could be extracted because of the uniform appearance of oil in the flow passage (unfortunately, the video graph or photograph of this pattern is not feasible and available). However, due to the drift in skewness from high to low value and the shift of the peaks, the flow could be described and referred to as the inversion point according to Jana et al. (2006b). In addition, this

region where the skewness drifts towards zero could also be referred to as a transition region in which the continuous phase changed from oil to water.

Table 8a: PDF description of oil-water flow at V_{so} 0.06m/s

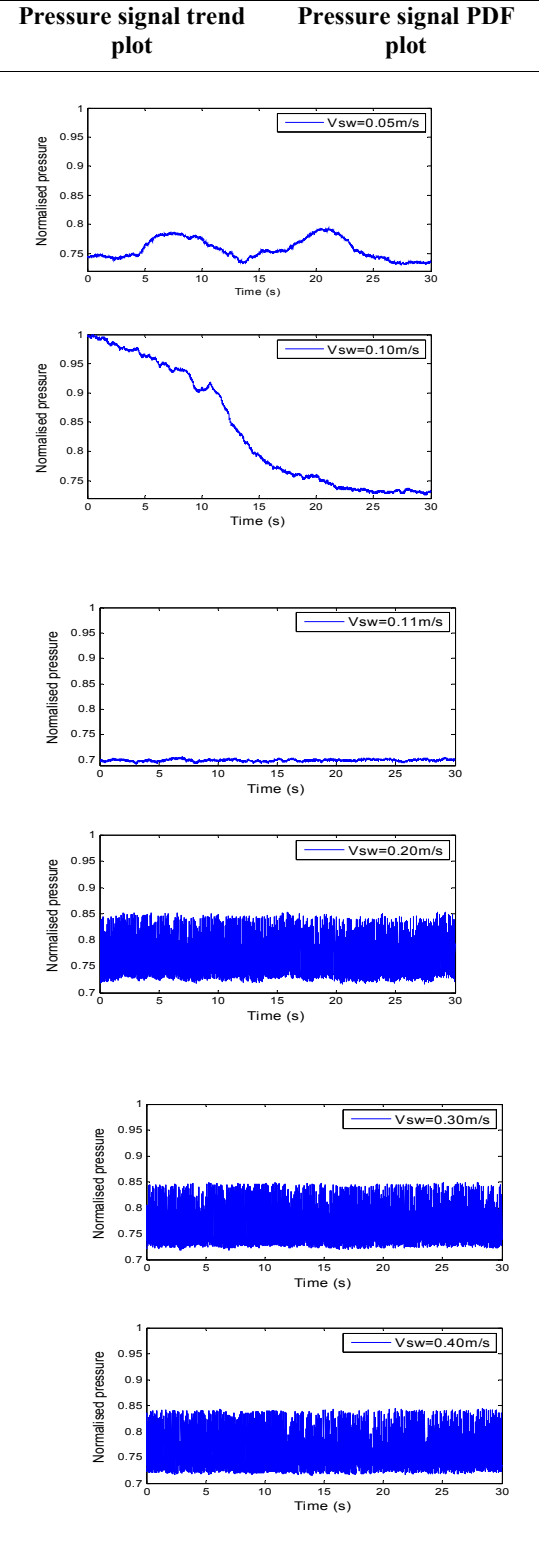
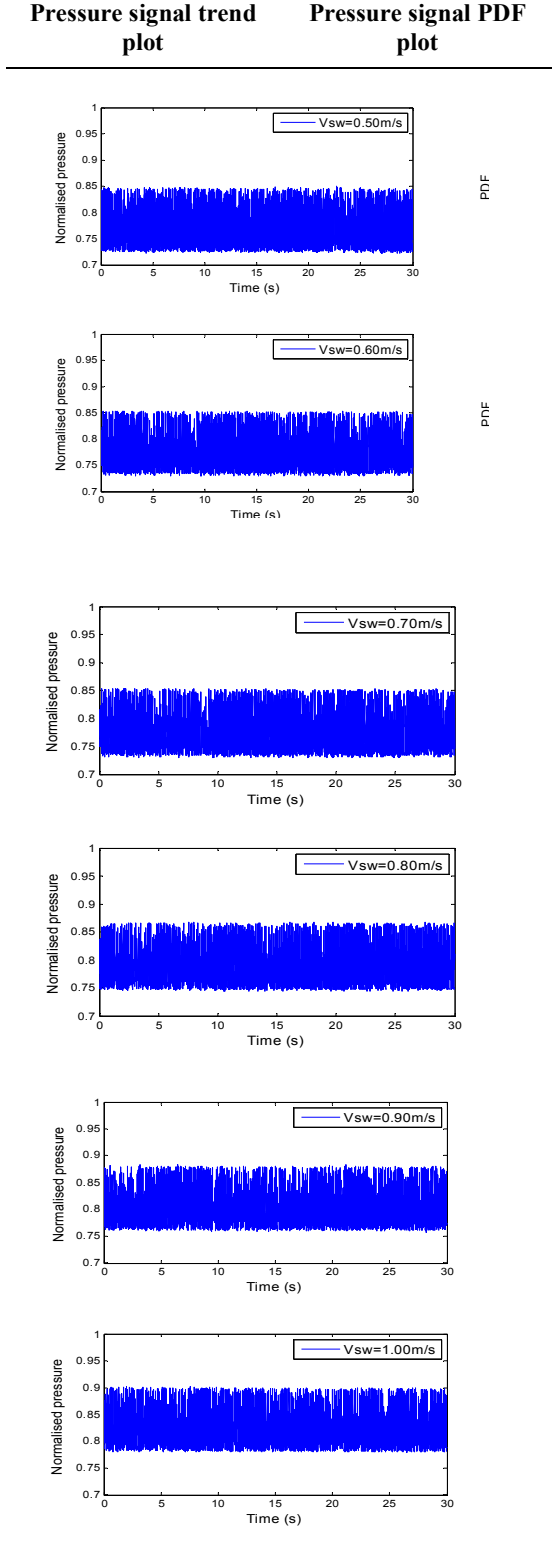


Table 9b: PDF description of oil-water flow at V_{so} 0.06m/s



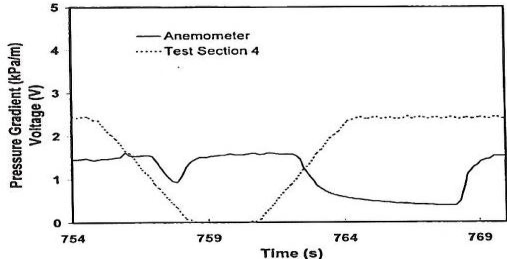


Figure 7: Anemometer profile ($r/R = 0.8, \theta = 0$) and pressure gradient result for mixture velocity $=0.038\text{m/s}$ with 10% water cut (McKibben et al., 2000)

A further increase in the V_{sw} from 0.11m/s upward results in more positive skewness, increase in standard deviation of the data and the kurtosis. As earlier mentioned, for V_{so} equals 0.06m/s and V_{sw} greater than 0.11m/s , OPW/OF and DOW/OF were observed, and WA-ANN when V_{so} equals 0.2m/s and 0.55m/s at V_{sw} greater than 0.10m/s and 0.15m/s , respectively. The spread of the base of the PDF curve in this region also suggests the oil film existence on the wall (as commonly refer in the PDF of gas-liquid flow that involves film on the pipe wall). In addition, the PDFs have two small peaks in addition to the main peak. This shows that the flow is intermittent. The spread of the distribution was relatively constant, showing the presence of oil film on the wall at high V_{sw} (i.e. beyond the oil continuous region).

In

Table 10, the V_{so} was fixed at 0.2m/s with V_{sw} varying from low to high. When the V_{sw} was 0.01m/s , a negative skew value with a standard deviation lower than unity was observed. It has broad distribution, but there is neither video nor photograph to conclude the description because the pipe was dominated by oil. When the water velocity increased to 0.03m/s , there was a shift in skewness to positive accompanied with the broad distribution and some peaks. These peaks suggest that increase in V_{sw} increases the intermittent behaviour, although oil was still the continuous (carrier) phase. When V_{sw} was increased to 0.05 and 0.1m/s the standard deviation reduced drastically with skewness dropping almost to zero. The thin peak PDF curve, as described above, suggests an inversion region. When the V_{sw} was increased above 0.1m/s , the skewness and kurtosis increased as well with PDF having two peaks, which suggests that the flow is intermittent. The behaviour of the flow when V_{so} equals 0.55m/s at varying V_{sw} was observed to be the same as observed in V_{so} equals 0.2m/s at varying V_{sw} . It could be deduced that higher V_{so} favours WA-ANN flow.

Table 10: PDF description of oil-water flow at $V_{so} 0.2\text{m/s}$

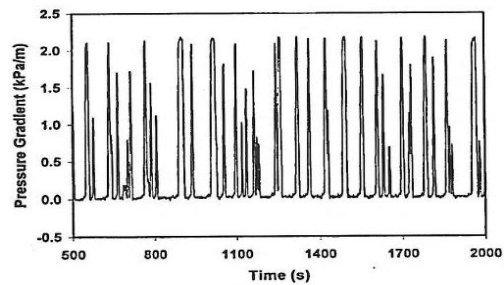
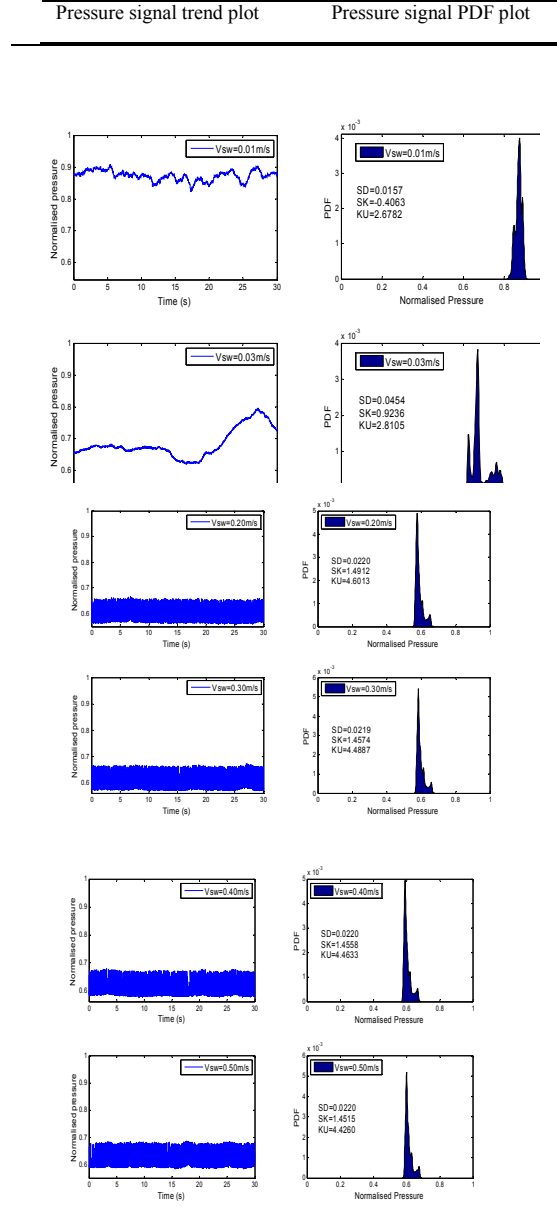


Figure 8: Instantaneous pressure gradient data at 67% water cut (McKibben et al., 2000)

Flow pattern map

Comparing some of the results obtained from the available visual observation with the trend plots and PDF distributions. The two-phase flow regime starts when the water cut or V_{sw} is greater than zero. The first flow pattern classification (i.e. WPO) was done purely based on the PDF and the pressure gradient because the video graph data did not reveal them as separated flows. Some behaviour that is classified as swirl water-oil (i.e. SWO) or transition actually has oil on the wall, while water and the core oil formed a spiral kind of movement as shown in Table 7. This kind of flow behaviour was observed to be inconsistent because it was not an enduring type throughout the pipe; it occurred randomly at different locations along the pipe unlike other flow patterns that existed continuously from the oil-water mixing point to the exit of the pipe. When the V_{sw} is increased, oil appeared as plug in the water continuous flow known as OPW and further increase of V_{sw} led to the dispersion of oil in the pipe called DOW. However, an increase in V_{so} promoted annular flow types which are identified as WA-ANN as specified in the maps below. All of these flow patterns have oil film on the wall except WPO where oil formed the continuous flow.

The comparison of the flow pattern maps of the present research with Sotgia et al. (2008) are as presented on Figure 10 to 11. Two maps were generated by Sotgia et al. (2008) based on the pipe materials; plexiglas and pyrex, and diameters; 26mm and 40mm respectively. The results of the present research are compared with the map developed from oil-water flow in 26mm Plexiglas horizontal pipe. Generally, it could be observed from Sotgia's map that good parts of WA-ANN are captured. In the case of slug/ annular flows transition boundary, the boundary exists when the oil flow rate is very low which quite agreed with the present study. However, stratified flows are not obtained in this investigation; perhaps, the variance observed in the map could be traced to the pipe material, or the oil properties used in these studies. Sotgia used mineral oil whose viscosity ratio to water is 900 and density ratio is 0.9 at 20°C, while the present research employs the viscosity ratio of about 3300 and density ratio of 0.924 at 20°C. In addition, their measured oil-water interfacial tension is 0.02, as against 0.026 and 0.029 in this research for CYL680 and CYL1000 respectively. It could be easily observed in the Figure9, Figure 110 and Figure 11 that the transition boundaries are functions of the properties of the mineral oils. The figures also show that Sotgia's flow map is not sufficient to predict very high viscosity oil. However, their boundary for slug-annular appear reasonable, although it is not accurate in all these figures.

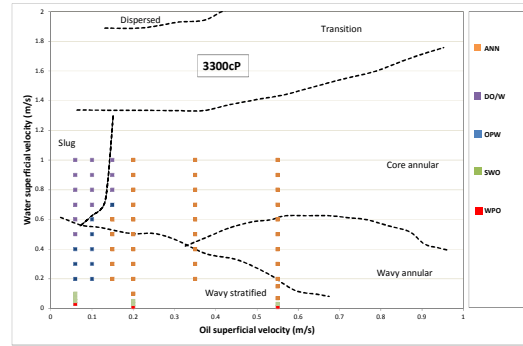


Figure 9: Comparing flow pattern of 3300cP oil and water with Sotgia et al [14] literature data

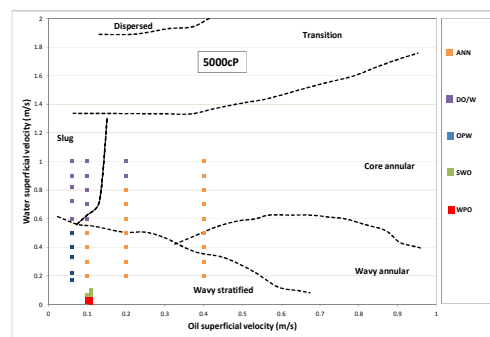


Figure 10: Comparing flow pattern of 5000cP oil and water with Sotgia et al (2008) literature data

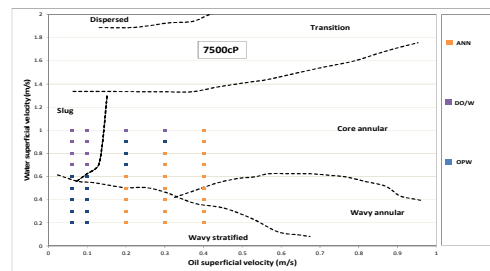


Figure 11: Comparing flow pattern of 7500cP oil and water with Sotgia (2008)

Conclusions

The superficial velocities of high viscosity oil and water strongly influenced both the pressure gradient and flow pattern of this multiphase flow. The flow pattern types were identified and reported from the visualisation (video) of the flow, description by the trend plot and PDF of the downstream pressure signals along with the statistical moments. The observed flow patterns are WPO, OPW/OF, WA-ANN, and DOW/OF.

Acknowledgements

The author would like to acknowledge the Petroleum Technology Development Programme (PTDF), Nigeria for their financial support on this project.

References

- Dusseault, M. (1993), "Cold Production and Enhanced Oil Recovery", *Journal of Canadian Petroleum Technology*, 32(9): 28-38.
- Dusseault, M., Geilikman, M. and Roggensack, W. (1995), "Practical requirements for sand production implementation in heavy oil applications", SPE International Heavy Oil Symposium. 19-21 June, Calgary, Alberta, Canada.
- Besson, C. (2005), *Resources to Reserves: Oil and Gas Technologies for the Energy Markets of the Future*, OECD Publishing.
- Owen, N. A., Inderwildi, O. R. and King, D. A. (2010), "The status of conventional world oil reserves—Hype or cause for concern?", *Energy Policy*, 38(8) :4743-4749.
- Barnea, D., Shoham, O. and Taitel, Y. (1980), "Flow pattern characterization in two phase flow by electrical conductance probe", *International Journal of Multiphase Flow*, 6(5):387-397.
- Martinez, A., Arirachakaran, S., Shoham, O. and Brill, J. (1988), "Prediction of Dispersion Viscosity of Oil/Water Mixture Flow in Horizontal Pipes", SPE Annual Technical Conference and Exhibition.
- Brauner, N. and Moalem Maron, D. (1992), "Flow pattern transitions in two-phase liquid-liquid flow in horizontal tubes", *International Journal of Multiphase Flow*, 18(1): 123-140.
- Trallero, J., Sarica, C. and Brill, J. (1997), "A study of oil-water flow patterns in horizontal pipes", *Old Production & Facilities*, 12(3):165-172.
- Angeli, P. and Hewitt, G. (2000), "Flow structure in horizontal oil-water flow", *International Journal of Multiphase Flow*, 26(7):1117-1140.
- Santoso B., Indarto, Deendarlianto and Widodo T. S. (2012) Differential pressure fluctuation of plug flow pattern gas-liquid of co-current two phase flow in a horizontal pipe. *Journal of Fluids and Thermal Sciences*, 1(2): 205-217.
- Joseph, D., Bai, R., Chen, K. and Renardy, Y. (1997), "Core-annular flows", *Annual Review of Fluid Mechanics*, 29(1):65-90.
- Arney, M. S., Ribeiro, G. S., Guevara, E., Bai, R. and Joseph, D. D. (1996), "Cement-lined pipes for water lubricated transport of heavy oil", *International Journal of Multiphase Flow*, 22(2): 207-221.
- Angeli, P. and Hewitt, G. (1999), "Pressure gradient in horizontal liquid-liquid flows", *International Journal of Multiphase Flow*, 24(7):1183-1203.
- Sotgia, G., Tartarini, P. and Stalio, E. (2008), "Experimental analysis of flow regimes and pressure drop reduction in oil-water mixtures", *International Journal of Multiphase Flow*, 34(12):1161-1174.
- Bensakhria, A., Peysson, Y. and Antonini, G. (2004), "Experimental study of the pipeline lubrication for heavy oil transport: Pipeline transportation of heavy oils= Ecoulement des bruts lourds dans les conduits", *Oil & gas science and technology*, 59(5): 523-533.
- Strazza, D., Grassi, B., Demori, M., Ferrari, V. and Poesio, P. (2011), "Core-annular flow in horizontal and slightly inclined pipes: Existence, pressure drops, and hold-up", *Chemical Engineering Science*, 66(12):2853-2863
- McKibben, M. J., Gillies, R. G. and Shook, C. A. (2000), "A laboratory investigation of horizontal well heavy oil—water flows", *The Canadian Journal of Chemical Engineering*, 78(4):743-751.
- Matsui, G. (1984), "Identification of flow regimes in vertical gas-liquid two-phase flow using differential pressure fluctuations", *International Journal of Multiphase Flow*. 10(6):711-719.
- Matsui, G. (1986), "Automatic identification of flow regimes in vertical two-phase flow using differential pressure fluctuations", *Nuclear Engineering and Design*,. 95:221-231.
- Jana, A. K., Das, G. and Das, P. K. (2006a), "A novel technique to identify flow patterns during liquid-liquid two-phase upflow through a vertical pipe", *Industrial & Engineering Chemistry Research*, 45(7): 2381-2393.
- Jana, A. K., Das, G. and Das, P. K. (2006b), "Flow regime identification of two-phase liquid-liquid upflow through vertical pipe", *Chemical Engineering Science*, 61(5): 1500-1515.